Wide-Ranging Equations of State for B_4C Constrained by Theoretical Calculations and Shock Experiments

S. Zhang,[1,2] M. C. Marshall,[1,2] L. H. Yang,[2] P. A. Sterne,[2] B. Militzer,[3] M. Däne,[2] J. A. Gaffney,[2] A. Shamp,[2] T. Ogitsu,[2] K. Caspersen,[2] A. E. Lazicki,[2] D. Erskine,[2] R. A. London,[2] P. M. Celliers,[2] J. Nilsen,[2] and H. D. Whitley[2]

[1]Laboratory for Laser Energetics, University of Rochester
[2]Lawrence Livermore National Laboratory
[3]Departments of Earth and Planetary Science and Astronomy, University of California, Berkeley

The design of high-energy-density (HED) and inertial confinement fusion (ICF) experiments requires a good description of the ablator equation of state (EOS). Currently, CH plastics are typically used as ablators, and their EOS has been extensively studied (see Fig. 1). However, the formation of condensed phase microstructures, species separation, and mixing with the DT fuel during an implosion could affect the performance of the ICF target or interpretation of HED experiments.[1–3] Other materials with higher densities and hardness, such as boron, have been explored as alternative ablators. In the past three years, we have combined various theoretical approaches with planar shock experiments and benchmarked the EOS of boron (B)[4] and boron nitride (BN)[5] over wide ranges of density–temperature conditions. Under constraints provided by these data, new *Purgatorio*-based EOS models (LEOS 50 for B and X52 for BN) have been constructed and made available for use in hydrodynamic simulations. As a follow-up, this work presents a comprehensive study of the EOS of boron carbide (B_4C), another important member in the family of boron materials.

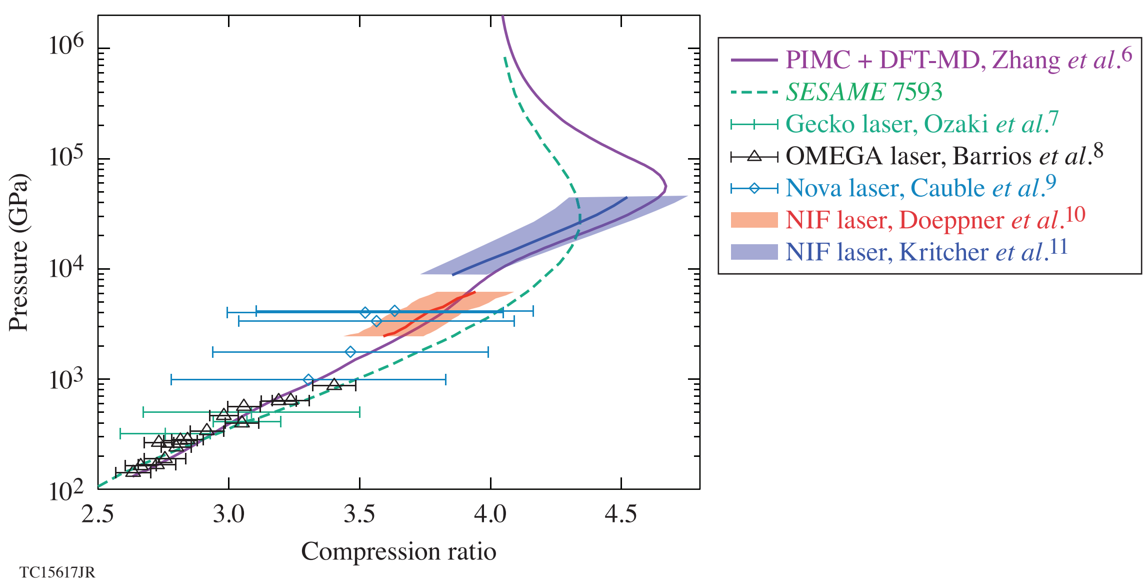

Figure 1
The Hugoniot of CH polystyrene from first-principles computations is consistent with planar shock experiments and verified by the latest spherically converging shock data at the National Ignition Facility (NIF). In comparison, the Thomas–Fermi-based *SESAME* 7593 model predicts the Hugoniot to be much smoother around the compression maximum and is invalidated by the NIF data. The initial sample density ρ_0 = 1.05 g/cm^3.

The computational methods that we have employed include path-integral Monte Carlo (PIMC) and density functional theory molecular dynamics (DFT-MD), which provide a wide-ranging, internally coherent first-principles EOS for B_4C in hot plasma, warm dense matter, and condensed liquid states. The calculations are jointly benchmarked by computations using an all-electron Green's function Korringa–Kohn–Rostoker (MECCA) and an activity expansion (ACTEX) approach. The theoretical predictions of the Hugoniot EOS are cross validated by comparisons with Hugoniot measurements up to 6100 GPa from planar shock experiments performed on the NIF.

Figure 2 summarizes the major findings of this research, including EOS comparisons between PIMC and DFT-MD, as well as Hugoniot comparisons between predictions by various computational methods or semi-empirical models and shock experiments. Note that our DFT-MD calculations have been performed in multiple ways, including one that uses projector augmented wave (PAW) potentials with plane-wave basis (PAWpw) and another one that uses optimized norm-conserving Vanderbilt (ONCV) potentials combined with pw basis or a Fermi-operator expansion. The PAW potentials have a frozen 1*s* core, which limits the PAWpw computations to temperatures below 5×10^5 K and moderately high densities (we considered up to 20.07 g/cm^3). We used all-electron ONCV potentials for calculations at temperatures up to 1.35×10^6 K and densities up to 50.18 g/cm^3. The EOS produced by the ONCV calculations matches both the PAWpw data at low temperatures and the PIMC data at high temperatures very well, as shown with overlapping isotherms in Fig. 2(a).

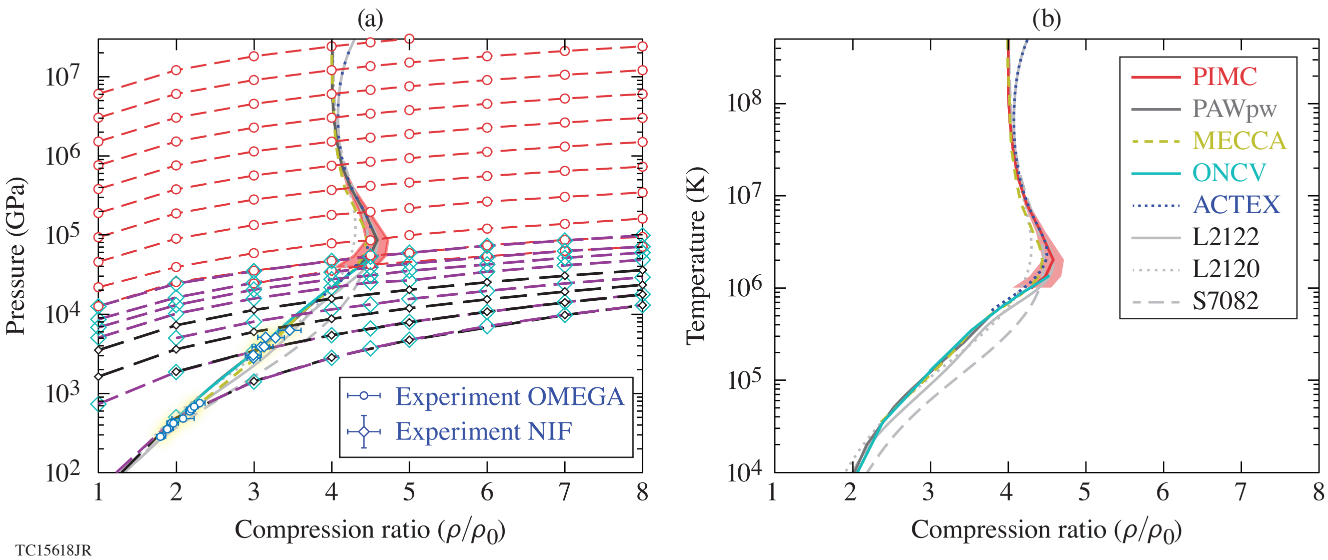

Figure 2
The (a) pressure–compression and (b) temperature–compression Hugoniot of B_4C from various computational methods (PIMC, PAWpw, ONCV, MECCA, and ACTEX) in comparison with predictions by different EOS models (L2122/2120: LEOS models; S7082: a *SESAME* model) and measurements by two separate laser shock experiments (OMEGA, by Fratanduono *et al.*,[6] and the NIF, this work). The initial sample density ρ_0 = 2.51 g/cm^3. The shaded area around the lower end of the PIMC Hugoniot curve represent 1σ uncertainty in the corresponding Hugoniot density due to EOS errors. In (a), EOS data along selective isotherms from three approaches are also shown with dashed lines and points (PIMC in red circles, ONCV in cyan diamonds, and PAWpw in small black diamonds). The lowest two isotherms for ONCV (and PAWpw) correspond to temperatures of 10^4 and 1.26×10^5 K, respectively. The highest two isotherms for ONCV (and the lowest two by PIMC) correspond to 1.01×10^6 and 1.35×10^6 K, respectively. The deviation between PIMC/L2120 (and MECCA) and ACTEX/L2122 Hugoniot curves above 106 GPa and 2×10^7 K is due to the electron relativistic effect, which is considered in ACTEX and L2122 but not in PIMC/L2120 (and not fully in MECCA).

Our calculated Hugoniot curves using the different theoretical approaches show good consistency with each other and overall agreement with two independent sets of experimental measurements at 200 to 6100 GPa. At the highest pressure of the OMEGA data[12] and the lowest pressure of the NIF data, our DFT-MD predictions of the Hugoniot are slightly stiffer than the experiment, which could be worthwhile to study in the future. Assisted by the theoretical predictions, we estimate the corresponding Hugoniot temperatures for the NIF data to be in the range of 1 to 5×10^5 K. Our Hugoniot results also show overall good consistency with the L2122 model and predict B_4C to have a maximum compression ratio of 4.55 at 9×10^4 GPa and 2×10^6 K, below which L2122 predicts B_4C to be slightly softer. In comparison, Thomas–Fermi model L2120 predicts B_4C at the compression maximum to be stiffer by ~6% and *SESAME* 7082 predicts B_4C to be much softer at pressures of 800 to 3×10^4 GPa.

We compared the EOS of B_4C between our first-principles predictions and L2122 and found a maximum pressure discrepancy of ~18% occurring at 6×10^3 to 2×10^5 K. We have therefore constructed three new EOS models (L2123 to 2125) by variations of the cold curve and the ion thermal EOS model to span the range of experimental error bars. We then performed a series of 1-D hydrodynamic simulations of direct-drive implosions with a B_4C ablator described by the four EOS models (L2122 to 2125) based on a polar-direct-drive exploding-pusher platform.[13–15] The results showed that the performance is insensitive to the EOS variations.

This material is based upon work supported by the Department of Energy National Nuclear Security Administration under Award Number DE-NA0003856, the University of Rochester, and the New York State Energy Research and Development Authority. This work was in part performed under the auspices of the U.S. Department of Energy by Lawrence Livermore National Laboratory under Contract No. DE-AC52-07NA27344.

1. D. S. Clark *et al*., Phys. Plasmas **23**, 056302 (2016).
2. S. Yu Gus'kov *et al*., J. Russ. Laser Res. **38**, 173 (2017).
3. S. Zhang and S. X Hu, Phys. Rev. Lett. **125**, 105001 (2020).
4. S. Zhang *et al*., Phys. Rev. E **98**, 023205 (2018).
5. S. Zhang *et al*., Phys. Rev. B **99**, 165103 (2019).
6. S. Zhang *et al*., J. Chem. Phys. **148**, 102318 (2018).
7. N. Ozaki *et al*., Phys. Plasmas **16**, 062702 (2009).
8. M. A. Barrios *et al*., Phys. Plasmas **17**, 056307 (2010).
9. R. Cauble *et al*., Phys. Plasmas **4**, 1857 (1997); R. Cauble *et al*., Phys. Rev. Lett. **80**, 1248 (1998).
10. T. Döppner *et al*., Phys. Rev. Lett. **121**, 025001 (2018).
11. A. L. Kritcher *et al*., Nature **584**, 51 (2020).
12. D. E. Fratanduono *et al*., Phys. Rev. B **94**, 184107 (2016).
13. C. L. Ellison *et al*., Phys. Plasmas **25**, 072710 (2018).
14. H. D. Whitley *et al*., "Comparison of Ablators for the Polar Direct Drive Exploding Pusher Platform," Physics Archive, https://arxiv.org/abs/2006.15635 (2020).
15. C. B. Yeamans *et al*., "High Yield Polar Direct Drive Fusion Neutron Sources at the National Ignition Facility," submitted to Nuclear Fusion.